

Calibration of Dynamic Volume-Delay Functions: A Rolling Horizon-Based Parsimonious Modeling Perspective

Yuyan Pan¹, Jifu Guo², and Yanyan Chen¹

Abstract

Volume-delay functions (VDF) are the critical building block in static traffic assignment and general demand-supply analysis. This paper aims to provide a rolling horizon-based modeling framework to establish and further calibrate dynamic VDF (DVDF) for a corridor. The development and application of classic VDF in recent traffic planning studies are first reviewed. Analytical formulas based on a rolling horizon framework are then developed to redefine critical elements in the Bureau of Public Roads (BPR) function to capture the time-dependent volume–delay relationship. Time-dependent average demand and discharge rate are used in a real-world bottleneck in oversaturated conditions. By constructing an estimate or approximate for the dynamic degree of saturation, the proposed method could (i) better interpret the underlying mechanism of the time-dependent demand–delay function; (ii) provide a valuable tool to estimate the speed for a time rolling horizon with given real-time data in practice, and (iii) analyze the correlation between a bottleneck and upstream or downstream on a road network to acquire accurate discharge rates for different situations. Experiments using corridors in Beijing and Los Angeles demonstrate that the proposed dynamic analytical methods can outperform the traditional BPR function in dynamic congestion cases. The results improve the DVDF goodness-of-fit from R^2 of 44% to 87% under different conditions, which sheds more light on future online traffic simulation applications.

Keywords

planning and analysis, transportation demand management, congestion mitigation, corridor management, dynamic travel

Real-time spatial-temporal information of traffic flow is widely available from loop detectors or probe vehicles (1). Static traffic assignment is usually referred to as the process of allocating the predicted origin–destination (OD) demand to the given network according to specific user behavioral principles (2). As one of the key elements of traffic assignment, volume-delay functions (VDF) is a mathematical expression that quantifies traffic impedance caused by demand volume (3). However, the traffic demand in the real-world traffic network evolves, requiring planners and engineers to fully recognize the traffic stream's dynamic characteristics. Therefore, static traffic assignment has been recognized as having the following limitations: (i) it cannot capture the time-dependent volume–delay relationship; (ii) the trip “desire” in the traffic assignment on a road could exceed the road's capacity, but the observed volume on a road usually cannot exceed its physical capacity (4); (iii) In the *Highway Capacity Manual*, levels of service (LOS) A to D

represent the uncongested traffic state and LOS F represents congested traffic state with demand greater than supply (5). VDF has difficulty modeling conditions in LOS F, so many researchers use the dynamic traffic assignment method to illustrate how congestion levels vary with time. On the other hand, simulation-based dynamic traffic assignment could be too complex to be implemented in a real-world, large-scale network. The above considerations motivated the authors to develop a parsimonious model that can systematically consider the traffic dynamics during the calibration of the VDF.

¹Beijing Key Laboratory of Traffic Engineering, Beijing University of Technology, Beijing, China

²Beijing Transport Institute, Beijing, China

Corresponding Author:

Yanyan Chen, cdyan@bjut.edu.cn

Transportation Research Record
 2022, Vol. 2676(2) 606–620
 © National Academy of Sciences:
 Transportation Research Board 2021
 Article reuse guidelines:
sagepub.com/journals-permissions
 DOI: 10.1177/03611981211044727
journals.sagepub.com/home/trr


VDF determines the travel time according to the volume-to-capacity ratio at the link level. A widely used VDF is the BPR (Bureau of Public Roads) function, which was proposed by the U.S. Bureau of Public Roads in 1964 (6). In general, VDF should be analyzed under different traffic conditions, such as free-flow state and congestion state. However, the volume in the bottleneck cannot be directly observed; therefore, traditional VDF cannot directly reflect the oversaturated condition. Meanwhile, VDF cannot capture the building up, dissipation, and spillback of queues. Some researchers, such as Huntsinger and Roushail (7), indicated that the modeled volume or, more precisely, “oversaturated demand” should be considered as the sum of a capacity term and residual queue. They provided a method to estimate and analyze queues in a bottleneck and resulting VDF function based on “demand over capacity” ratios.

There are also other methods of considering dynamic oversaturated conditions in a bottleneck. As a typical rolling horizon-based approach, Kalman filtering (KF) forecasts congestion propagation in a bottleneck location. It can provide a middle-term forecast for days with recurrent and non-recurrent traffic conditions (8). However, typical KF methods mainly rely on speed measurements in this traffic state estimation field, and they do not directly estimate the average discharge rate in a bottleneck. As a result, this study has the following research goals: (i) based on Huntsinger and Roushail’s method, to combine the rolling horizon-based method and VDF to better represent the time-dependent demand in a bottleneck and (ii) to explore the correlation between upstream and downstream in a bottleneck, to acquire accurate dynamic discharge rate for different traffic states. The proposed dynamic analytical methods are demonstrated with two case studies: a freeway corridor in Los Angeles and congested highway segments on the West-Third-Ring of Beijing.

Literature Review

Traditional VDF

VDFs have been widely used in static traffic assignment and general demand-supply analysis. Blunden (9) summarized three noteworthy features related to VDF: (i) the travel time at the link is close to free-flow travel time when the capacity is sufficient; (ii) slow change of flow rate will lead to the slight change of travel time when the observed volume on the roads is far less than the road capacity; (iii) in the stable state of traffic flow, the travel time curve will become an asymptote of the saturated flow ordinate. The widely used BPR function is recognized as an analytical building block for system-wide performance evaluation, as shown as Equation 1:

$$tt = t_f \left[1 + \alpha \left(\frac{q}{c} \right)^\beta \right] \quad (1)$$

where

tt = the link travel time,

t_f = the travel time at the free-flow speed,

q = volume,

c = the capacity of the link or segment,

α, β = the parameters related to volume over capacity ratio.

The parameter α is the ratio of travel time per unit distance at practical capacity to a free-flow state. The parameter β determines how abruptly the curve drops from the free-flow speed. Many practitioners suggested the values of 0.15 and 4 for α and β , respectively (10).

The simplicity of the BPR function is a critical reason for its widespread use. Since the BPR function was established on highway data under uncongested conditions in its early deployment stage, the results for highly congested segments might not accurately reflect the real-world traffic flow condition (11–13). These limitations led planners and engineers to modify BPR curves to match local travel activities (14–22).

Dynamic VDF

Many successful models of dynamic VDF have been widely developed. Nam and Drew (23) developed a dynamic traffic flow model for estimating freeway travel time from flow measurements taken at upstream and downstream stations. Vanajakshi et al. (24) proposed several modifications to an existing traffic flow theory-based model on the freeway. Moreover, Yi and Williams (25) presented a modified dynamic traffic flow model for accurately estimating the travel time of freeway links under a congestion condition. Li et al. (26) designed a new algorithm to describe the fast travel time variations between upstream and downstream detectors to reduce the error between the upstream and downstream sensors. There have been several studies in combination with emerging technologies to capture dynamic volume–delay relationships. Ke et al. (27) proposed a deep learning approach to address three dependencies within one end-to-end learning architecture. Wu et al. (28) proposed a computational graph framework to capture hierarchical travel demand with different data sources.

Link travel time estimation could be generally divided into four major categories in Table 1. This paper proposes a rolling horizon-based demand over capacity method in a bottleneck to calibrate the time-dependent VDF.

Some methods involving queueing analysis have also been used to estimate the VDF. Kucharski and Drabicki (3) employed a fundamental diagram to derive the quasi-

Table 1. Comparison of Different Models and Their Features

Publication	Approach	Input and output	Features
Ahmed and Cook (29)	Statistical methods	Input: q, k, v Output: lane-based static average travel time	Estimate local traffic conditions for route guidance, adaptive ramp metering, and signal control.
Cremer and Papageorgiou (30)	Macroscopic traffic flow models	Input: q, k, v Output: link-based static average travel time	Estimate traffic flow, density, and queue length on each link.
Peeta and Mahmassani (31)	Dynamic-link travel time function	Input: q, k, v Output: link-based dynamic travel time	Estimate current traffic states and provide future network traffic states.
Huntsinger and Roushail (7)	Dynamic queue-based model	Input: q, k, v Output: queue-based dynamic travel time	Consider demand as a sum of queued flow and capacity.
This paper	Time-dependent flow-based model	Input: q, k, v Output: average travel time/speed for the rolling horizon	Estimate real-time demand and supply in a congestion condition.

density form from measured time-mean speeds and flows. The quasi-density method is shown in Equation 2:

Method A: Quasi-Density Method (3). Quasi-density (QD) is used here as a substitute for flow, while the density-at-capacity $k(q_{max})$ (namely, critical density k_c) substitutes the capacity at any time.

$$q = \frac{k}{k(q_{max})} \cdot c \quad (2)$$

However, the traditional BPR function is mainly used to measure the general level-of-service traffic conditions for traffic systems, and it is challenging to use it to capture instantaneous traffic conditions. Within the subject of analytical dynamic traffic assignment modeling, as reviewed in Peeta and Mahmassani (31), the immediate link travel time model is widely adopted to describe link travel time. Furthermore, such a model is typically a simple nonlinear time-dependent “whole-link” model without exponents, as in Equation 1. The instantaneous link travel time is built on the time-dependent inflow and outflow rate in a link.

Method B: Time-Dependent Traffic Flow Method (32). Within the subject of analytical dynamic traffic network analysis, the “whole-link” model is widely adopted to describe link travel time evolution because of its simple description of traffic flow propagation through an analytical form, as in Equation 3.

$$x(t) = q(t-1) + \int_0^t [u(\tau) - v(\tau)] d\tau \quad (3)$$

where $x(t)$ is the number of flows on the link at time t , $q(t-1)$ is the queue at the previous time interval $t-1$, and $u(\tau)$ and $v(\tau)$ are time-dependent inflow and outflow rates at time t .

Although the time-dependent link travel time function models provides some degree of simplification in travel time analysis, there is one significant limitation. Traffic congestion usually occurs at some bottleneck, and queues are produced and often grow beyond the bottleneck, which makes it difficult for some travel time functions to capture the duration and spatial impact of congestion.

Method C: Demand Beyond Capacity on the Bottleneck Method (7). Among numerous methods, Huntsinger and Roushail provided a time-dependent queue-based D/c model (TDQDC) for estimating demand beyond capacity, $v/c > 1$, as shown in Equation 4. This model proposed a hypothesis that average bottleneck travel time is a nonlinear function based v/c , and it follows the seven rules proposed by Spiess (11).

$$demand(t) = c + queue(t) \quad (4)$$

where $demand(t)$ is an average measure of queued demand and capacity at time t , c is ultimate capacity, and $queue(t)$ is the spatial extent of a queue at time t , which is equal to the density at time interval t for a detector multiplied by area of influence for a detector. This $queue(t)$ concept is derived from the traffic flow theory by May (33). This model is a straightforward nonlinear regression to calibrate exponents, and it used the empirical study to calibrate capacity. It has not shown a further connection with theoretical queueing models.

VDF, such as the BPR function, have been widely used in static traffic assignment. VDF mainly recognized as an analytical function for system-wide performance evaluation. However, since it is based on highway data under uncrowded conditions, the results obtained in practice cannot accurately reflect the actual situation, especially in the oversaturated situation, in which demand exceeds capacity. Compared with the static traffic assignment model, the dynamic traffic assignment (DTA) model aims to embed a queueing model or other types of dynamic traffic flow models to capture the evolution processes of traffic congestion. This study is motivated by developing analytical formulas to capture the time-dependent volume–delay relationship, especially for the flow regime in which demand exceeds capacity. This approach is made possible by the availability of reliable freeway traffic surveillance data and explores the correlation between upstream and downstream in a bottleneck.

Calibration Method of Rolling Horizon-Based VDF

Considering a bottleneck, given numerous observed speed, flow, and occupancy data, this section focuses on estimating the following three key parameters: (i) average travel time/speed across the dynamic period; (ii) virtual waiting queue at simulation time t ; and (iii) physical queue and waiting time at time t from a virtual queue, at time t . As queueing is a complex process, this study is particularly interested in determining the variation of demand over time and considering the spatial characteristics of the queue itself. To describe the relationship between virtual queue, spatial queue, and physical queue, the corridor bottleneck with a constant maximum capacity (or discharge rate μ) is first considered. Second, it is assumed that a constant free-flow speed v_f holds for all uncongested traffic (independent of flow), and that whenever congestion occurs upstream of the bottleneck, vehicles traverse the queue at some constant speed v_μ (dependent on the bottleneck flow and derived from the $q - k$ curve function), which is lower than the free-flow speed. It is also assumed that speed changes occur instantaneously. Finally, it is assumed that vehicles neither enter nor leave the traffic stream in the queue and between the adjacent sequence.

The waiting time in the queue is denoted as $w(t)$, and the free-flow travel time is represented as t_f leading to the following equation:

$$d(t) = v_f \cdot t_f = v_\mu \cdot (t_f + w(t)) \quad (5)$$

Then we can obtain the following equation, as demonstrated by Lawson et al. (34):

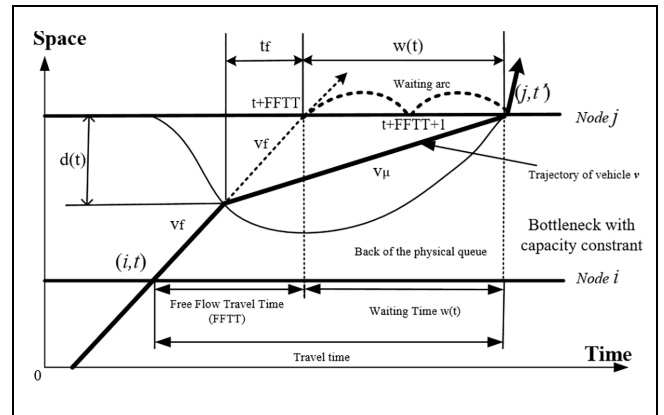


Figure 1. Vehicle trajectory with a bottleneck in the space–time network.

Source: From Lawson et al. (34).

$$d(t) = \frac{v_\mu \cdot w(t)}{1 - \frac{v_\mu}{v_f}} \quad (6)$$

Furthermore, to strike a balance between the model and limited data coverage to approximate traffic states in real-world freeway corridors, this research adopts the simplified queueing model proposed by Lawson et al. (34). Further, it integrates with the deterministic fluid approximation model proposed by Newell (35) for comparative estimation of macroscopic traffic states at the bottleneck level. Along this line, one can extend the method by Lawson et al. to calculate the spatial and temporal extents of the queue and the actual waiting time spent upstream of a bottleneck.

The schematic trajectories of vehicle v from node i to node j in a space–time network are shown in Figure 1. Consider a physical transportation network $M = (N, L)$ with a finite set of nodes N and links L , where nodes $i, j \in N$, and directed link $(i, j) \in L$. The study by Lu et al. (36) provides a more systematic comparison among modes of point queues, spatial queues, and an extended version with time-dependent capacity and queue spillover along with the backward wave.

It is also assumed that the arrival rate $\lambda(t)$ is a polynomial function. It is easy to see that the inflow rate $\lambda(t)$ is a derivative of the cumulative arrival curve $A(t)$ and the discharge rate $\mu(t)$ is a derivative of the cumulative departure curve $V(t)$. Let us denote t_0 and t_3 as the times at which the queue generates and dissipates, respectively, which leads to the virtual waiting queue at simulation time t :

$$Q^v(t) = A(t) - V(t) = w(t) \cdot \mu(t) = \int_{t_0}^t [\lambda(\tau) - \mu(\tau)] d\tau, t \in [t_0, t_3] \quad (7)$$

The variable of interest is now the physical queue at time t from a virtual queue at time t :

$$Q^p(t) = \frac{d(t)}{v_\mu} \cdot \mu(t) = \frac{\mu(t) \cdot w(t)}{1 - \frac{v_\mu}{v_f}} = \frac{Q^v(t)}{1 - \frac{v_\mu}{v_f}}, t \in [t_0, t_3] \quad (8)$$

Many link performance measures can be used to evaluate the service quality of an oversaturated system, such as delay, queue length, or congestion period. Cheng et al. (37) denote D as demand from time t_0 to t_3 , denote μ as the average discharge rate during this congestion period; thus, D/μ is the expression for congestion period P . In this paper, $D(\tau)$ means cumulative demand during time interval τ , $\mu(\tau)$ represents the discharge rate during time interval τ . In the proposed rolling horizon framework that aims to estimate $D(\tau)/\mu(\tau)$ dynamically, we consider an approximation as shown in Equation 9.

$$\frac{D}{\mu} = \frac{D(\tau)}{\mu(\tau)}, \tau \in [t_0, t_3] \quad (9)$$

To calibrate the BPR function in each peak period, other regression methods give one sample point with multiple data samples using multiple links over different days. However, this paper only studies the individual link, and each rolling stage gives one sample point. The number of data samples corresponds to periods over a 24 h day, or 6:00 a.m.–6:00 p.m., again for this link only. Link-specific but dynamic travel time function is based on the time-dependent $D(\tau)/\mu(\tau)$ loading factor for each rolling stage. This research further considered both congested and uncongested locations and then proposed the following Method D.

Method D: Time-Dependent Cumulative Demand Flow-Based Travel Time Method (TDCD). By substituting Equation 9 into Equation 1, for the individual link only, each rolling horizon gives one sample point.

$$q/c = \begin{cases} \frac{q}{c}, & \text{if } t \in \text{uncongested period} \\ \frac{D(\tau)}{\mu(\tau)}, & \text{if } t \in \text{congested period} \end{cases} \quad (10)$$

The rolling horizon framework in this paper follows the system design of a dynamic traffic assignment system (38–40). The scheme entails sequential execution of the flow estimator and predictor in conjunction with real-time simulators. Furthermore, the rolling horizon solution framework successfully solves each demand sub-horizon and carries over any finished demand to the following sub-horizon. As shown in Figure 2, the horizon starts at the end of a rolling period, the time shift between the respective beginning of consecutive prediction horizons. As is shown in Figure 2, it is necessary to

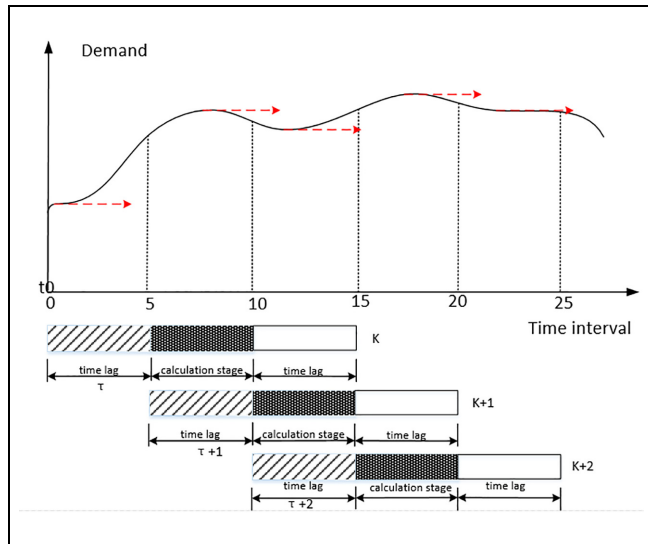


Figure 2. Illustration of rolling horizon implementation.

Table 2. Notations and Explanations Used in this Paper

Notations	Explanations
t_0	The start time of the congestion period
t_3	The end time of the congestion period
tt	Total travel time
t_f	Free-flow travel time
v_f	Free-flow speed
v_μ	Congestion flow speed
P	Congestion period, $P = t_3 - t_0$
$\lambda(t)$	Inflow rate at time t
μ	Outflow rate at time t (constant discharge rate)
$\mu(\tau)$	Discharge rate during time interval τ
$w(t)$	Traffic delay at time t
$A(t)$	Cumulative arrival curve at time t
$D(\tau)$	Cumulative demand during time interval τ
$V(t)$	Cumulative departure curve at time t
$Q^v(t)$	Virtual queue length at time t
$Q^p(t)$	Physical queue length at time t
$\text{demand}(t)$	Demand at time t
q	Flow rate
c	Capacity
D	Demand
k	Rolling horizon iteration
τ	Time interval

calculate dynamic cumulative demand $D(\tau)$ and moving average discharge $\mu(\tau)$ in each time interval. The rolling horizon implementation of calibration time-dependent VDF is termed “Procedure 1,” and the notations used in this paper are shown in Table 2.

The input of this procedure is a combination of measurements q, k, v , with the output as average travel time/speed for the rolling horizon.

Procedure I. Rolling horizon implementation for calibration of dynamic volume-delay functions

- Step 1: Receive real-time traffic measurements from a surveillance system, such as a loop detector.
 Step 2: According to the cut-off speed v_c or critical density k_c to find the start time of the congestion period t_0 and the end time of the congestion period t_3 on the rolling horizon.
 Step 3: Estimate time-dependent demand $D(\tau)$ involved in the current estimation stage.
 Step 4: Estimate time-dependent moving average discharge rate $\mu(\tau)$ involved in the current estimation stage.
 Step 5: Calculate the time-dependent demand over-discharge rate $D(\tau)/\mu(\tau)$ in the current rolling horizon.
 Step 6: Calibration parameters according to proposed TDCCD using the least square fit method.
 Step 7: Advance rolling horizon forward from k to $k + 1$.
-

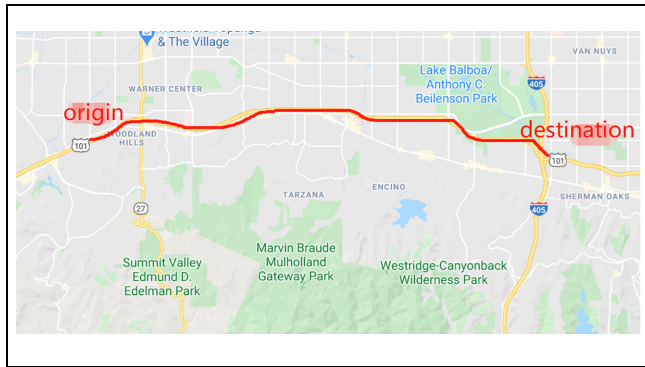


Figure 3. Los Angeles corridor used for data acquisition.

Case Study

Traffic Data Description

Case 1: Los Angeles. The data used for validating the proposed TDCCD model were obtained using loop detectors on July 1, 2019 (Monday) on a corridor, Absolute Postmile (Abs) 18.907 to 24.032, on the US101-S freeway in Los Angeles, California from the open-access PeMS (2013) database. Raw data consisted of flows, roadway occupancies, and spot speeds aggregated at an interval of 5 min for each mainline lane. Equation 12 was used to convert occupancy data into density data. A schematic diagram of the study section is presented in Figure 3. Figure 4 shows the speed contour map of the corridor; detector 19.432 is the location of the bottleneck. Detailed descriptive information about the detectors is listed in Table 3.

$$k = \frac{5280 * Occ}{l + d} \quad (11)$$

where Occ is occupancy, l is the average length of the vehicle, and d is the average area of influence for a detector.

Reasonableness checks included a review of flow-speed, density-flow, and density-speed plots based on the 5 min flow rates. Figure 5 provides sample plots of

these relationships, which reflect classic traffic flow characteristics as expected.

Case 2: Beijing. The data used for validating the proposed TDCCD model were obtained using loop detectors on June 1, 2018 (Monday) from 6:00 a.m. to noon on a corridor on the West-Third-Ring of Beijing, China. Raw data consisted of flows and spot speeds aggregated at intervals of 2 min for each mainline lane. As $q = kv$, density data are indirectly calculated from the speed and flow measurements. A schematic diagram of the study section is presented in Figure 6. Figure 7 shows the speed contour map of the corridor, and we can observe that detector HI2090c is the location of the bottleneck. Table 3 offers related details.

Figure 8 shows the plots of flow-speed, density-flow, and density-speed relationships, which reflect classic traffic flow characteristics as expected.

Model Validation

With the increase of crowding, traffic flow decreases. In this case, the impedance function such as Equation 1 is less likely to be suitable for calculating impedance. The following different models are now used to obtain parameter y in Equation 13:

$$v = \frac{v_f}{[1 + \alpha(y)^B]} \quad (12)$$

1. The proposed TDCCD method

$$y = \begin{cases} \frac{q}{c}, & \text{if } t \in \text{uncongested period} \\ \frac{D(\tau)}{\mu(\tau)}, & \text{if } \tau \in \text{congested period} \end{cases} \quad (13)$$

2. QD method

QD is used here as a substitute for the flow, while the density-at-capacity $k(q_{max})$ (equal to the critical density k_c) substitutes the capacity.

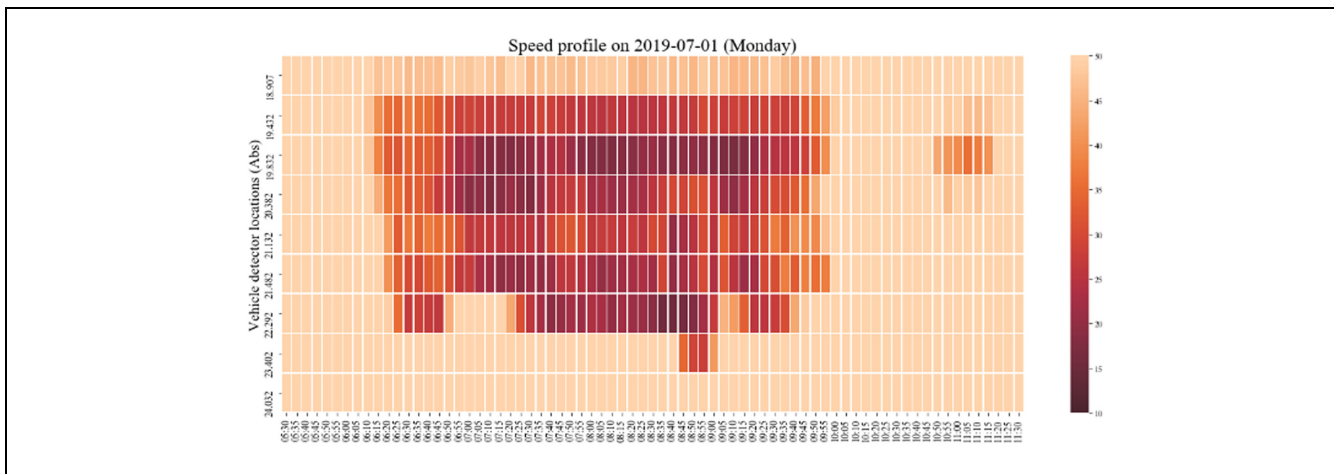


Figure 4. Speed contour map of the Los Angeles corridor.

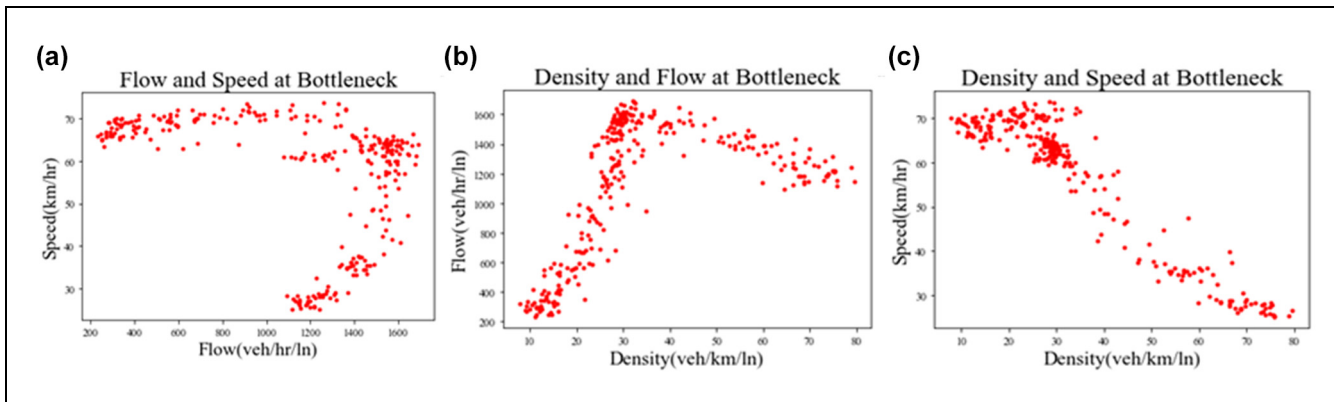


Figure 5. Fundamental flow–speed–density relationships at bottleneck on Los Angeles corridor: (a) flow–speed relationship, (b) density–flow relationship, and (c) density–speed relationship.

Table 3. Descriptive Information of Detectors

Los Angeles case

Detector ID	Absolute mile	Number of lanes	Length (mile)	Detector ID	Absolute mile	Number of lanes	Length (mile)
1	18.907	6	0.4325	6	21.482	5	0.58
2	19.432	6	0.4625	7	22.292	5	0.96
3	19.832	5	0.475	8	23.402	5	0.87
4	20.382	5	0.65	9	24.032	5	0.575
5	21.132	5	0.55				

Beijing West-Third-Ring case

Detector ID	Name	Number of lanes	Length (mile)	Detector ID	Name	Number of lanes	Length (mile)
1	HI2092c	2	500	6	HI8064c	3	512
2	HI2090c	3	1653	7	HI8027c	4	1157
3	HI8030c	3	1093	8	HI8026c	3	587
4	HI2065c	3	924	9	HI8025c	4	746
5	HI2063c	3	777				

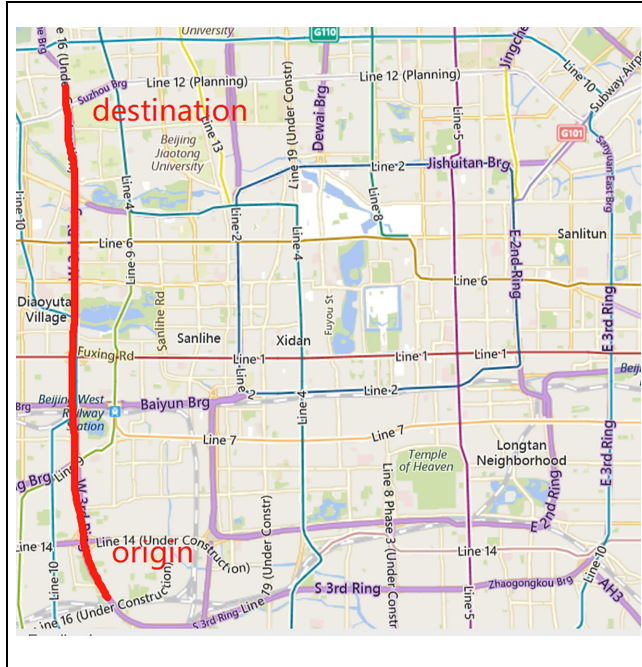


Figure 6. Beijing corridor used for data acquisition.

$$y = \frac{k}{k(q_{max})} \quad (14)$$

3. Huntsinger and Roushail's TDQDC method

One of the challenges of using data observed in the field to calibrate VDF is measuring demand when it exceeds capacity.

$$y = \begin{cases} \frac{q}{c}, & \text{if } t \in \text{uncongested period} \\ \frac{D(t)}{c}, & \text{if } t \in \text{congested period} \end{cases}, \quad \text{demand}(t) = c + \text{queue}(t) \quad (15)$$

Results and Discussion

Estimation of Time-Dependent Discharge Rate

Many existing travel time estimation methods assume the homogeneity of traffic flow. However, when widespread moving jams appear, this simplification often leads to inaccurate estimates. As a result, when congestion occurs between the upstream and downstream detectors, the existing travel time estimation methods could obtain a significantly biased estimation. As a result, it is crucial to explore the correlation between upstream and downstream detectors and bottleneck and upstream/downstream detectors. Furthermore, the correlation between upstream and downstream sensors could also directly affect the average discharge rate μ at each location.

Case 1: Los Angeles and Case 2: Beijing

As shown in Figure 9, there is a high correlation between bottleneck and upstream/downstream detectors in Los Angeles, which indicates that the flow of the artery road is hardly affected by the on/off ramp. Moreover, the discharge rate among those detectors may be very close, even though they belong to different locations. However, Figure 10 depicts a significantly low correlation between bottleneck and upstream/downstream

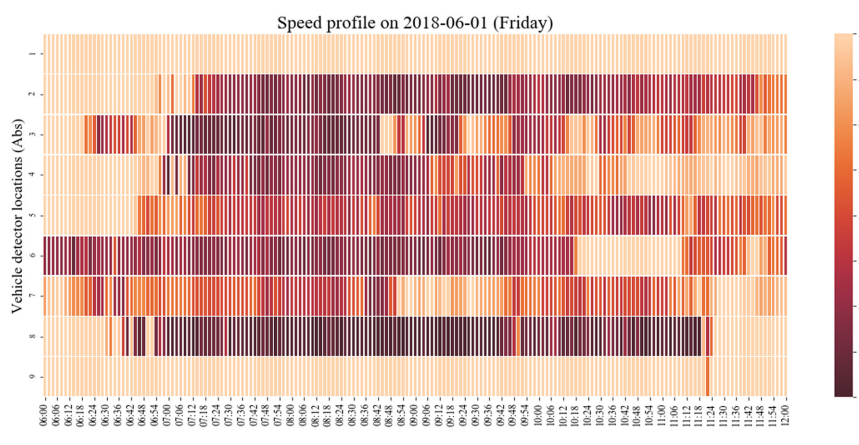


Figure 7. Speed contour map of the Beijing corridor.

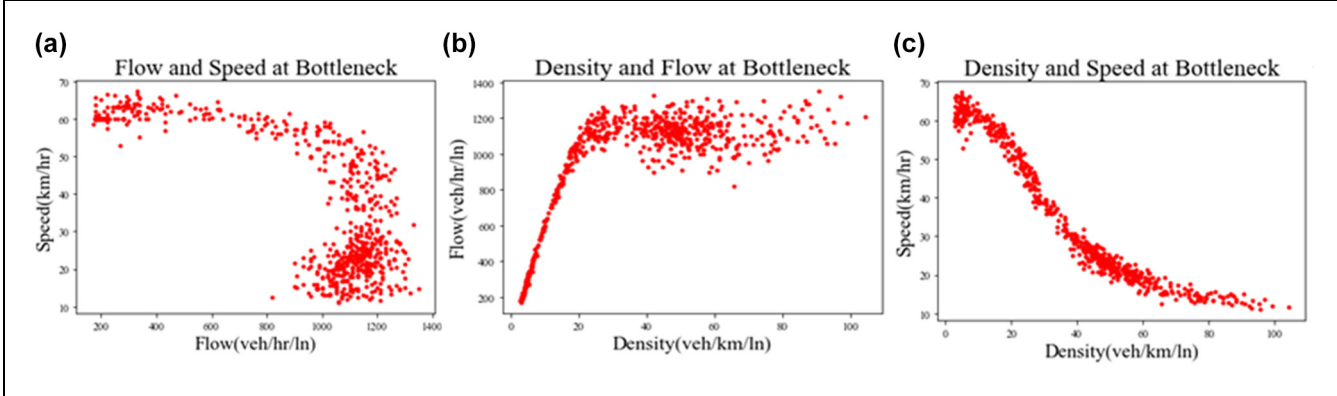


Figure 8. Fundamental flow–speed–density relationships at bottleneck on Beijing corridor: (a) flow–speed relationship, (b) density–flow relationship, and (c) density–speed relationship.

detectors in Beijing, and they even show a negative correlation relationship. In other words, it indicates that the flow of the artery road is not only affected by the on/off ramp but is also influenced by queue spillback, wave propagation, capacity drop, or some unobserved conditions. In this situation, it is necessary to estimate each detector's discharge rate at different periods. Analysis from microcosmic traffic behavior shows that in Los Angeles the traffic flow is relatively stable, there are fewer on/off ramps, and the driver behavior is relatively standard and cooperative. Consequently, its upstream and downstream traffic flow is more correlated. However, in Beijing, drivers' driving behavior is competitive and aggressive. It is greatly influenced by the on/off ramp on the road, so the traffic flow between upstream and downstream is less correlated.

Quality Checking

Regardless of the VDF type, a realistic reflection of the observed behaviors in a demand forecasting study requires a calibration process. In this section, two statistical measures are employed to quantify the effectiveness of these models: mean absolute error (MAE) and relative mean absolute error (RMSE). If N is the number of measurements, the calculation method of these two measures is given in Equations 18 and 19 as follows, respectively:

$$MAE = \frac{1}{N} \sum |measured - estimated| \quad (16)$$

$$RMSE = \sqrt{\sum \frac{(measured - estimated)^2}{N}} \quad (17)$$

In the travel demand models, highway traffic assignment requires a VDF with suitable parameters under free-flow speed and oversaturated conditions. In particular, only two parameters are to be determined in the BPR

function, and we simply need carefully to define and calibrate the ratio of q/c in Equation 1.

Case 1: Los Angeles case and Case 2: Beijing case

In this research, four models are applied to estimate the parameter settings of the BPR function. When the traffic flow condition is uncongested, we still use q/c . On the other hand, when the traffic flow condition is congested, the q/c is modified instead. The value of capacity c in Equation 1 is defined here as the practical capacity, which corresponds to the service volume at level of service C or about 80% of the maximum capacity of the facility (15).

In the TDCD method, the time-dependent value of $D(\tau)/\mu(\tau)$ is used to replace q/c . In the QD method, k/k_c is replaced with q/c in the oversaturated situation. In the TDQDC method, D is represented as the demand at a bottleneck. The recommended approach borrows the concept of measuring demand at the oversaturated signalized intersections. The vehicle queue plus the flow discharging at the stop line becomes a measure of the overall demand. As shown in Tables 4 to 5, we can conclude that the TDCD and QD methods have better performance than the other methods. QD method uses the quasi-density method from measured time-mean speeds and flows. QD and TDQDC methods both have goodness-of-fit in RMSE, correlation, MAE, and R^2 . However, the QD method cannot represent dynamic traffic phenomena like queue, spillback, wave propagation, and so forth. As a good supplement, the TDQDC model could describe the time-varying average demand and discharge rate by the proposed time-dependent demand–delay function in a congestion situation. Besides, Figure 11 intuitively shows the observed and estimated speed of the Los Angeles dataset, using different models, while Figure 12 further demonstrates the calibrated volume–delay curves of the



Figure 9. Correlations between bottleneck detector 19.432 and upstream or downstream detectors in Los Angeles case.



Figure 10. Correlations between bottleneck detector HI2090c and upstream or downstream detectors in Beijing case.

Table 4. Calibrated Parameters and Sensitivity Analysis Using Different Models in Los Angeles Case

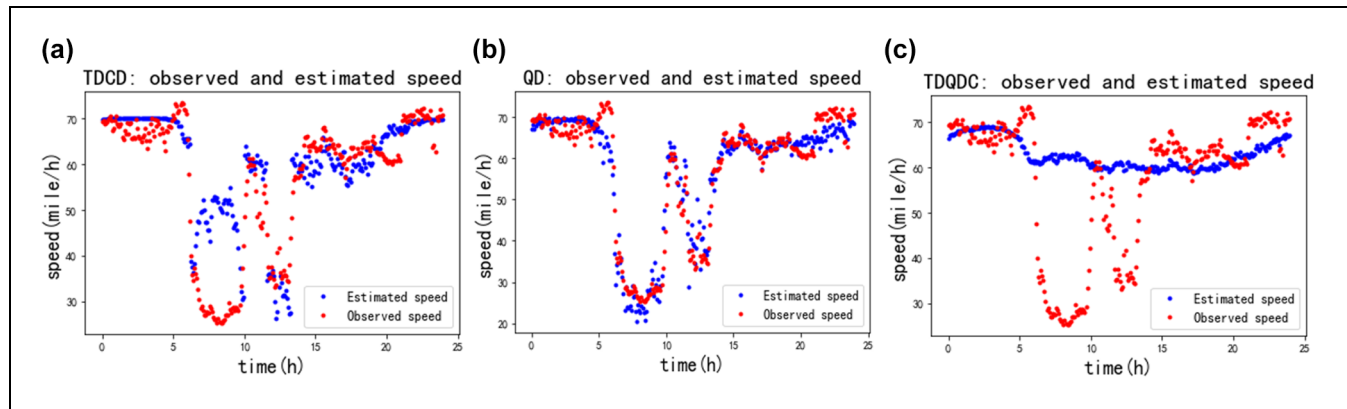
Method	Alpha	Beta	RMSE	Correlation	MAE	R-square
TDCD	0.15	4	8.595	0.822	6.301	0.6760
	0.08	5.74	8.971	0.820	5.890	0.6731
QD	0.15	4	7.683	0.970	5.418	0.9409
	0.12	3.09	3.920	0.965	2.885	0.9309
TDQDC	0.15	4	15.257	0.270	10.303	0.0726
	0.14	1.38	15.104	0.378	9.728	0.1426

Note: TDCD = time-dependent cumulative demand; QD = quasi-density; TDQDC = time-dependent queue-based demand/capacity; RMSE = relative mean absolute error; MAE = mean absolute error.

Table 5. Calibrated Parameters and Sensitivity Analysis Using Different Models in Beijing Case

Method	Alpha	Beta	RMSE	Correlation	MAE	R-Square
TDCD	0.15	4	7.079	0.930	5.498	0.8654
	0.37	2.57	5.311	0.934	3.973	0.8718
QD	0.15	4	10.175	0.937	8.347	0.8776
	0.73	1.92	2.186	0.989	1.767	0.9781
TDQDC	0.15	4	30.669	0.602	27.974	0.3618
	1.36	3.66	11.210	0.669	7.826	0.4480

Note: TDCD = time-dependent cumulative demand; QD = quasi-density; TDQDC = time-dependent queue-based demand/capacity; RMSE = relative mean absolute error; MAE = mean absolute error.

**Figure 11.** Comparison between the observed speed and estimated using different methods in Los Angeles case. (a) TDCD method; (b) QD method; (c) TDQDC method.

Los Angeles dataset. At the same time, Figures 13 and 14 describe the speed and volume–delay curves of the Beijing case, respectively.

Conclusion

The proposed analytical formulas are built on a rolling horizon framework to establish and further calibrate dynamic VDF for congested corridors. This study is intended to offer the following research results: (i)

propose an analytical method to interpret the underlying mechanism of dynamic demand–delay function; (ii) explore the correlation between upstream and downstream in a bottleneck, to estimate the speed for a time rolling horizon with given loop detectors.

The proposed method significantly improves estimates of delay and travel speeds compared with the existing VDF model. The approach documented in this paper could support planners in their wish for locally calibrated dynamic VDFs. The data analysis required is relatively

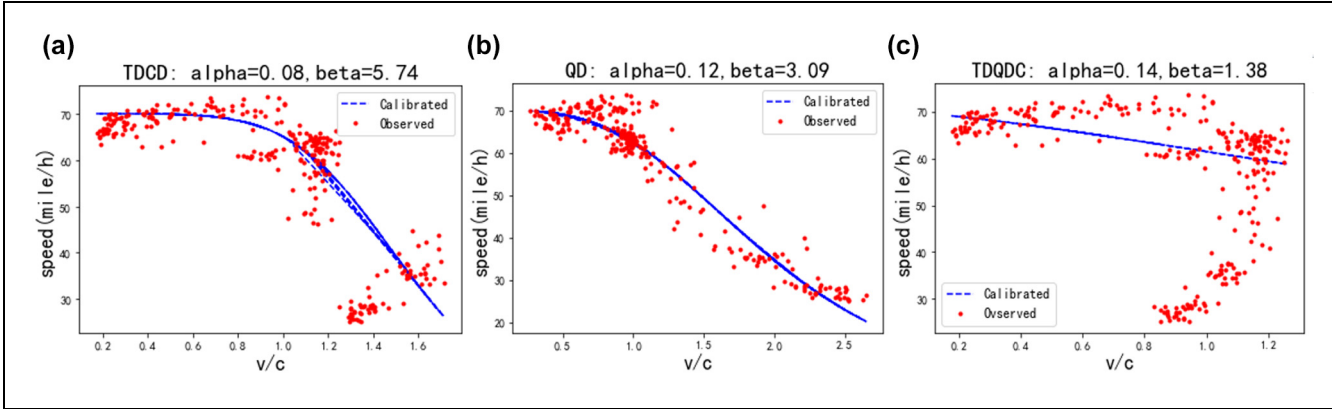


Figure 12. Calibrated speed curves of the different methods in Los Angeles case. (a) TDCD method; (b) QD method; (c) TDQDC method.

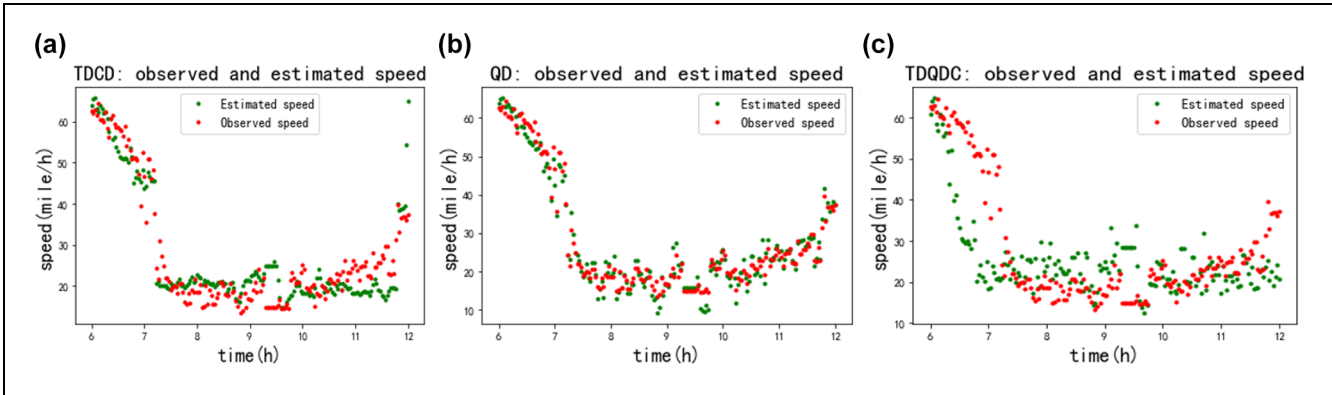


Figure 13. Comparison between the observed speed and estimated speed using different methods in Beijing case. (a) TDCD method; (b) QD method; (c) TDQDC method.

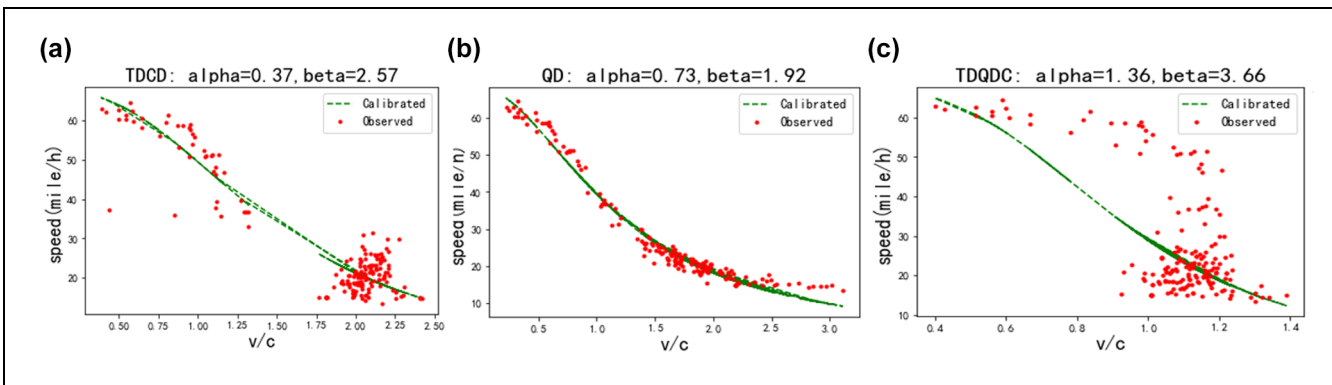


Figure 14. Calibrated speed curves of the different methods in Beijing case. (a) TDCD method; (b) QD method; (c) TDQDC method.

straightforward, with the demonstrated performance from two case studies. The authors believe that the static traffic assignment model with improved VDF is still effective for medium- or long-term traffic planning. In contrast, the dynamic volume-delay model should be

used to analyze time-varying phenomena such as traffic in peak period hours.

In the future, a spatial queue-based model will be studied to analyze more detailed traffic flow characteristics, such as queue spillback. The online modeling

framework could also be applied and extended to other emerging transportation applications under real-time and distributed computation environments.

Acknowledgments

The authors would like to thank Dr Xuesong (Simon) Zhou, Dr Xin (Bruce) Wu at Arizona State University, Dr Qixiu Cheng at Southeast University, and Dr Yongxiang Zhang at Southwest Jiaotong University for their excellent comments and assistance on our experiments.

Author Contributions

The authors confirm contribution to the paper as follows: study conception and design: Y. Pan, J. Guo, Y. Chen; data collection: Y. Pan; analysis and interpretation of results: Y. Pan, J. Guo; draft manuscript preparation: Y. Pan, Y. Chen. All authors reviewed the results and approved the final version of the manuscript.

Declaration of Conflicting Interests

The author(s) declared no potential conflicts of interest with respect to the research, authorship, and/or publication of this article.

Funding

The author(s) received no financial support for the research, authorship, and/or publication of this article.

References

1. Polson, N. G., and V. O. Sokolov. Deep Learning for Short-Term Traffic Flow Prediction. *Transportation Research Part C: Emerging Technologies*, Vol. 79, 2017, pp. 1–17.
2. Sheffi, Y. *Urban Transportation Networks: Equilibrium Analysis with Mathematical Programming Methods*. Prentice-Hall, Englewood Cliffs, NJ, 1984.
3. Kucharski, R., and A. Drabicki. Estimating Macroscopic Volume Delay Functions with the Traffic Density Derived from Measured Speeds and Flows. *Journal of Advanced Transportation*, Vol. 32, 2017, pp. 1–10.
4. Petrik, O., F. Moura, and J. A. de Silva. The Influence of the Volume-Delay Function on Uncertainty Assessment for a Four-Step Model. In *Computer-Based Modelling and Optimization in Transportation* (J. F. de Sousa and R. Rossi, eds.), Springer, Cham, 2014, pp. 293–306.
5. *Highway Capacity Manual 2010*. Transportation Research Board of the National Academies, Washington, D.C., 2010.
6. Bureau of Public Roads. *Traffic Assignment Manual*. Urban Planning Division, U.S. Department of Commerce, Washington, D.C., 1964.
7. Huntsinger, L. F., and N. M. Rouphail. Bottleneck and Queuing Analysis: Calibrating Volume-Delay Functions of Travel Demand Models. *Transportation Research Record: Journal of the Transportation Research Board*, 2011. 2255: 117–124.
8. Zhou, X., and H. S. Mahmassani. A Structural State Space Model for Real-Time Traffic Origin–Destination Demand Estimation and Prediction in a Day-to-Day Learning Framework. *Transportation Research Part B: Methodological*, Vol. 41, No. 8, 2007, pp. 823–840.
9. Blunden, W. R. *The Land-Use/Transport System: Analysis and Synthesis*. Pergamon Press, Oxford, 1971.
10. Branston, D. Link Capacity Functions: A Review. *Transportation Research*, Vol. 10, No. 4, 1976, pp. 223–236.
11. Spiess, H. Conical Volume-Delay Functions. *Transportation Science*, Vol. 24, No. 2, 1990, pp. 153–158.
12. Dowling, R. G., R. Singh, and C. W. Wei-Kuo. Accuracy and Performance of Improved Speed-Flow Curves. *Transportation Research Record: Journal of the Transportation Research Board*, 1998. 1646: 9–17.
13. Skabardonis, A., and R. Dowling. Improved Speed-Flow Relationships for Planning Applications. *Transportation Research Record: Journal of the Transportation Research Board*, 1997. 1572: 18–23.
14. Dowling, R., and A. Skabardonis. Improving the Average Travel Speeds Estimated by Planning Models. *Transportation Research Record: Journal of the Transportation Research Board*, 1993. 1360: 68–74.
15. Helali, K., and B. Hutchinson. Improving Road Link Speed Estimates for Air Quality Models. *Transportation Research Record: Journal of the Transportation Research Board*, 1994. 1444: 71–78.
16. Data Management Group. *Road Network Coding Manual*. Joint Program in Transportation, University of Toronto, 1991.
17. Irawan, M. Z., T. Sumi, and A. Munawar. Implementation of the 1997 Indonesian Highway Capacity Manual (MKJI) Volume Delay Function. *Journal of the Eastern Asia Society for Transportation Studies*, Vol. 8, 2010, pp. 350–360.
18. Davidson, K. B. A Flow Travel Time Relationship for Use in Transportation Planning. *Proc., 3rd Australian Road Research Board (ARRB) Conference*, Sydney, 1966.
19. Davidson, K. B. The Theoretical Basis of a Flow-Travel Time Relationship for Use in Transportation Planning. *Australian Road Research*, Vol. 8, No. 1, 1978, pp. 32–35.
20. Akcelik, R. A New Look at Davidson's Travel Time Function. *Traffic Engineering & Control*, Vol. 19, No. 10, 1978, pp. 459–463.
21. Akcelik, R. Travel Time Functions for Transport Planning Purposes: Davidson's Function, its Time Dependent Form and Alternative Travel Time Function. *Australian Road Research*, Vol. 21, No. 3 1991, pp. 49–59.
22. Smock, R. An Iterative Assignment Approach to Capacity Restraint on Arterial Networks. *Highway Research Board Bulletin*, No. 347, 1962, pp. 60–66.
23. Nam, D. H., and D. R. Drew. Automatic Measurement of Traffic Variables for Intelligent Transportation Systems Applications. *Transportation Research Part B: Methodological*, Vol. 33, No. 6, 1999, pp. 437–457.
24. Vanajakshi, L. D., B. M. Williams, and L. R. Rilett. Improved Flow-Based Travel Time Estimation Method from Point Detector Data for Freeways. *Journal of Transportation Engineering*, Vol. 135, No. 1, 2009, pp. 26–36.
25. Yi, T., and B. M. Williams. Dynamic Traffic Flow Model for Travel Time Estimation. *Transportation Research*

- Record: *Journal of Transportation Research Board*, 2015. 2526: 70–78.
26. Li, L., X. Chen, Z. Li, and L. Zhang. Freeway Travel-Time Estimation Based on Temporal-Spatial Queueing Model. *IEEE Transactions on Intelligent Transportation Systems*, Vol. 14, No. 3, 2013, pp. 1536–1541.
27. Ke, J., H. Zheng, H. Yang, and X. M. Chen. Short-Term Forecasting of Passenger Demand under On-Demand Ride Services: A Spatio-Temporal Deep Learning Approach. *Transportation Research Part C: Emerging Technologies*, Vol. 85, 2017, pp. 591–608.
28. Wu, X., J. Guo, K. Xian, and X. Zhou. Hierarchical Travel Demand Estimation Using Multiple Data Sources: A Forward and Backward Propagation Algorithmic Framework on a Layered Computational Graph. *Transportation Research Part C: Emerging Technologies*, Vol. 96, 2018, pp. 321–346.
29. Ahmed, M. S., and A. R. Cook. Analysis of Freeway Traffic Time-Series Data by Using Box-Jenkins Techniques. *Transportation Research Record: Journal of the Transportation Research Board*, 1979. 722: 1–9.
30. Cremer, M., and M. Papageorgiou. Parameter Identification for a Traffic Flow Model. *Automatica*, Vol. 17, No. 6, 1981, pp. 837–843.
31. Peeta, S., and H. S. Mahmassani. Multiple User Classes Real-Time Traffic Assignment for Online Operations: A Rolling Horizon Solution Framework. *Transportation Research Part C: Emerging Technologies*, Vol. 3, No. 2, 1995, pp. 83–98.
32. Lei, H., X. Zhou, G. F. List, and J. Taylor. Characterizing Corridor-Level Travel Time Distributions Based on Stochastic Flows and Segment Capacities. *Cogent Engineering*, Vol. 2, No. 1, 2015, p. 990672.
33. May, A. D. *Traffic Flow Fundamentals*. Prentice-Hall, Englewood Cliffs, NJ, 1990.
34. Lawson, T. W., D. J. Lovell, and C. F. Daganzo. Using Input-Output Diagram to Determine Spatial and Temporal Extents of a Queue Upstream of a Bottleneck. *Transportation Research Record: Journal of the Transportation Research Board*, 1997. 1572: 140–147.
35. Newell, C. *Applications of Queueing Theory*. Springer Science & Business Media, Berlin, Heidelberg, 2013.
36. Lu, C. C., J. Liu, Y. Qu, S. Peeta, N. M. Rouphail, and X. Zhou. Eco-System Optimal Time-Dependent Flow Assignment in a Congested Network. *Transportation Research Part B: Methodological*, Vol. 94, 2016, pp. 217–239.
37. Cheng, Q., Z. Liu, and X. S. Zhou. A Multiscale Demand and Supply Model for Oversaturated Dynamic Transportation Queueing Systems. 2020. https://www.researchgate.net/publication/338535980_A_multiscale_demand_and_supply_model_for_oversaturated_dynamic_transportation_queueing_systems/citations.
38. Mahmassani, H. S., T. Y. Hu, S. Peeta, and A. Ziliaskopoulos. *Development and Testing of Dynamic Assignment and Simulation Procedure for ATIS/ATMS Applications*. DTFH61-90-R-00074-FG. U.S. Department of Transportation, Federal Highway Administration, McLean, VA, 1994.
39. Mahmassani, H. S. Dynamic Network Traffic Assignment and Simulation Methodology for Advanced System Management Applications. *Networks and Spatial Economics*, Vol. 1, No. 3–4, 2001, pp. 267–292.
40. Huynh, N., H. S. Mahmassani, and H. Tavana. Adaptive Speed Estimation Using Transfer Function Models For Real-time Dynamic Traffic Assignment Operation. *Transportation Research Record: Journal of Transportation Research Board*, 2002. 1783: 55–65.